

## Supplementary Information

### Towards a Better Understanding of the Forming and Resistive Switching Behavior of Ti-Doped HfO<sub>x</sub> RRAM

Fabia F. Athena<sup>1</sup>, Matthew P. West<sup>2</sup>, Jinho Hah<sup>2</sup>, Riley Hanus<sup>3</sup>, Samuel Graham<sup>2,3</sup>, and Eric M. Vogel<sup>1,2\*</sup>

<sup>1</sup>School of Electrical and Computer Engineering, Georgia Institute of Technology, Atlanta, Georgia 30332, USA

<sup>2</sup>School of Materials Science and Engineering, Georgia Institute of Technology, Atlanta, Georgia 30332, USA

<sup>3</sup>George W. Woodruff School of Mechanical Engineering, Georgia Institute of Technology, Atlanta, Georgia 30332, USA

\*Email: eric.vogel@mse.gatech.edu

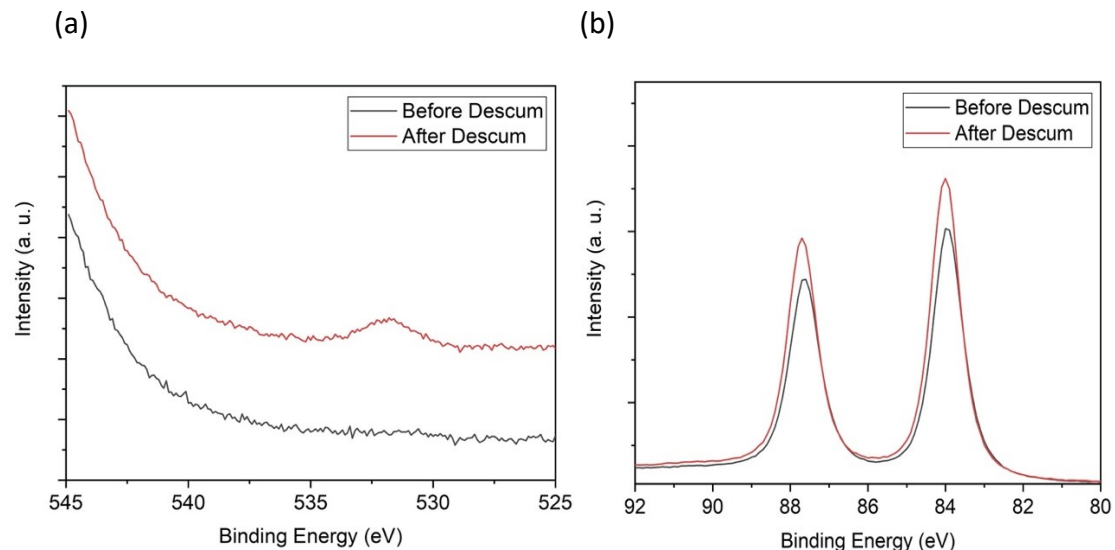
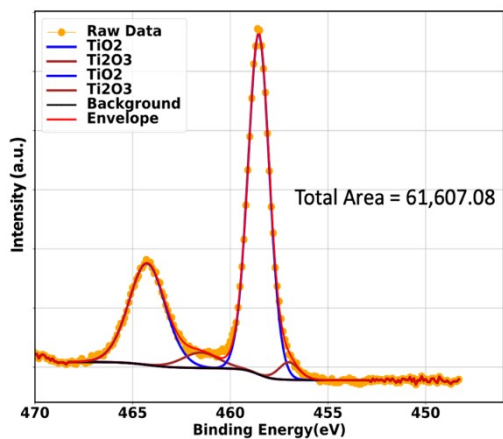


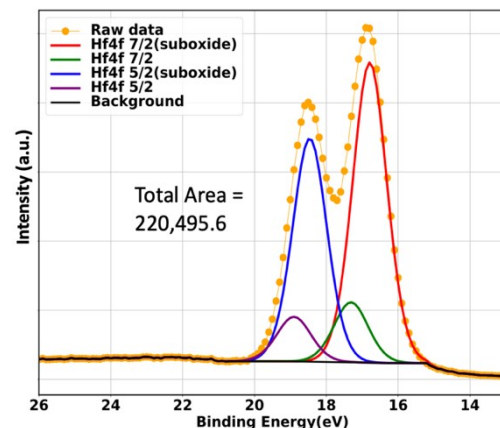
**Figure S1. High-resolution XPS (a) O 1s spectra and (b) Au 4f spectra before and after 30-sec descum procedure. Metallic Au, Au (0), is observed at 84.0 eV with no signs of Au(I) and Au (III) after the descum process. The presence of a small peak at 531.7 eV can be observed from O<sub>2</sub> plasma descum sample. The calculated oxygen area (%) is ~1.1 % which does not notably impact the oxidation state of Au significantly.**

From the XPS survey, the area percentage of carbon, oxygen and gold on the descum treated gold sample are 143183.00, 67135.88, and 5725569.74, respectively. The area % of the oxygen on the descum treated gold sample is =  $67135.88 / (143183.00 + 5725569.74) \approx 1.1\%$ .

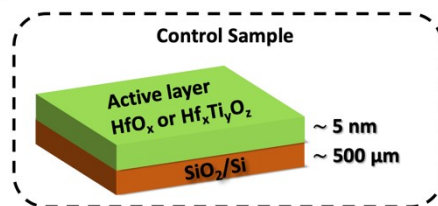
(a) Ti 2p Scan



(b) Hf 4f Scan



(c)



(d)

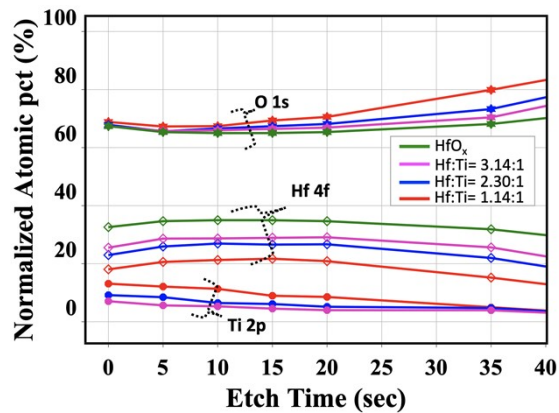


Figure S2: XPS fitting of Hf 4f and Ti 2p peaks of Hf<sub>x</sub>Ti<sub>y</sub>O<sub>z</sub> film used for the devices. (a) Ti 2p scan, (b) Hf 4f scan. The sensitivity factors used were 1.8 and 2.05 for titanium and hafnium, respectively. This results in Hf and Ti ratio 3.14: 1. (c) Schematics of the control sample having ~ 5 nm adaptive oxide used for XPS measurement fabricated along with the devices. (d) XPS depth profile of HfO<sub>x</sub> and Hf<sub>x</sub>Ti<sub>y</sub>O<sub>z</sub> showing the atomic percentage of Hf, Ti and, O elements at different etch levels. Ti is doped into the HfO<sub>x</sub> matrix uniformly in all of the samples.

## Calculation of x, y and z of $\text{Hf}_x\text{Ti}_y\text{O}_z$ :

**Table S1:** Exemplary calculation for Hf:Ti= 3.14:1 sample

Parameter	Hafnium	Titanium	Oxygen
Sensitivity factor (sf)	2.05	2.001	0.66
Peak area	220495.57	61607.08	172911.52
Peak/sf	107558.815	30788.1459	261987.152
Stoichiometry	$x = 0.26867262$	$y = 0.07690613$	$Z = 0.65442125$
Ratio $z/(x+y)$	1.89369647		

**Table S2:** Stoichiometry for all samples:

Sample	Stoichiometry
Hf: Ti = 1:0	$\text{HfO}_{1.91}$
Hf: Ti = 3.14:1	$\text{Hf}_{0.27}\text{Ti}_{0.07}\text{O}_{0.654}$
Hf: Ti = 2.3:1	$\text{Hf}_{0.253}\text{Ti}_{0.095}\text{O}_{0.65}$
Hf: Ti = 1.14:1	$\text{Hf}_{0.196}\text{Ti}_{0.16}\text{O}_{0.64}$

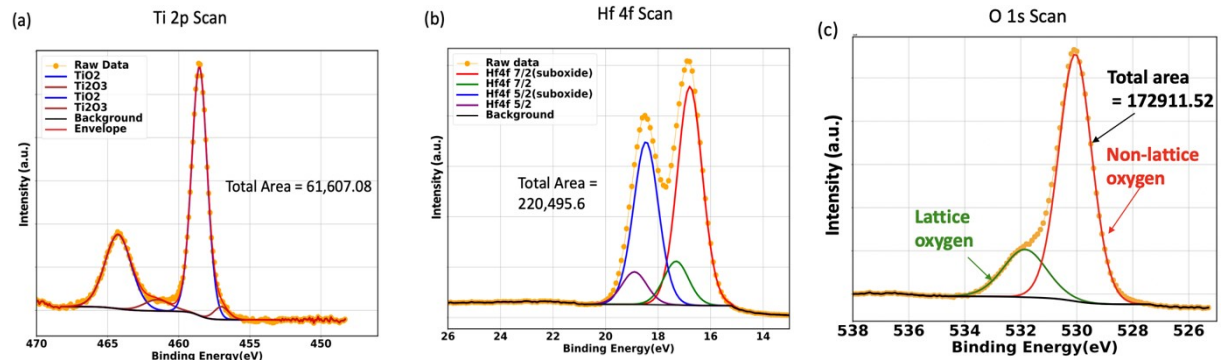


**Figure S3:** Stoichiometry analysis of and ratios for Hf:Ti= 3.14:1 sample. (a) Ti 2p scan, (b) Hf 4f scan. (c) O 2p scan. The sensitivity factors used were 1.8, 2.05 and 0.66 for titanium, hafnium and oxygen, respectively.

## XPS depth profile of $\text{HfO}_x$ and $\text{Hf}_x\text{Ti}_y\text{O}_z$ oxides:

Figure S2 shows depth profile of O 1s Hf 4f C 1s Si 2p and Ti 2p elements of  $\text{HfO}_x$  and  $\text{Hf}_x\text{Ti}_y\text{O}_z$  oxides control sample. These control samples were prepared and post processed in the same experimental conditions that were used for the devices.

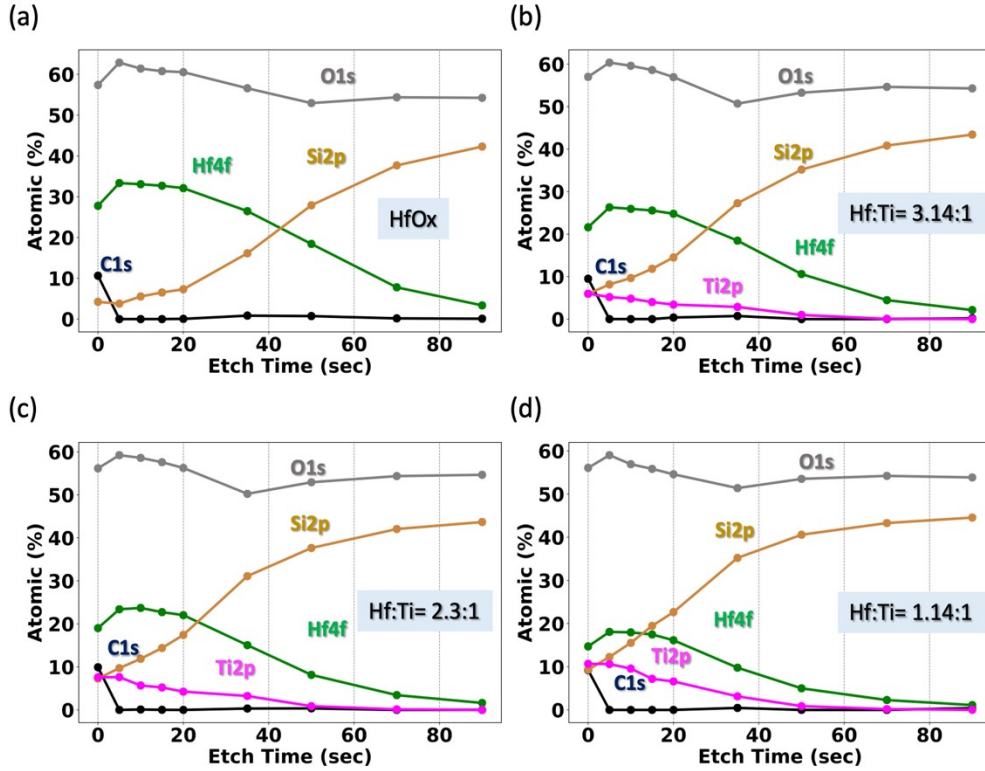


Figure S4: XPS depth profile of  $HfO_x$  and  $Hf_xTi_yO_z$ , showing atomic percentage of different elements at different etch levels. (a)  $HfO_x$ , (b)  $Hf:Ti = 3.14:1$ , (c)  $Hf:Ti = 2.3:1$  and, (d)  $Hf:Ti = 1.14:1$ .

### Forming current voltage relationship fitting with direct tunneling model:

Direct tunneling model, representing the relationship between current density and barrier height, is as follows-

$$J_D = \frac{A V^2}{\left[1 - \left(\frac{\Phi_B - qV}{\Phi_B}\right)^2\right]^{1/2}} \exp\left(-\frac{392}{V} \Phi_B^{3/2}\right)$$

Trap-assisted-tunneling model, representing the relationship between current density and barrier height, is as follows-

$$J_{TAT} = A \exp\left(-\frac{8\pi t o \chi \sqrt{2 q m^*}}{3hV} \Phi_T^{3/2}\right)$$

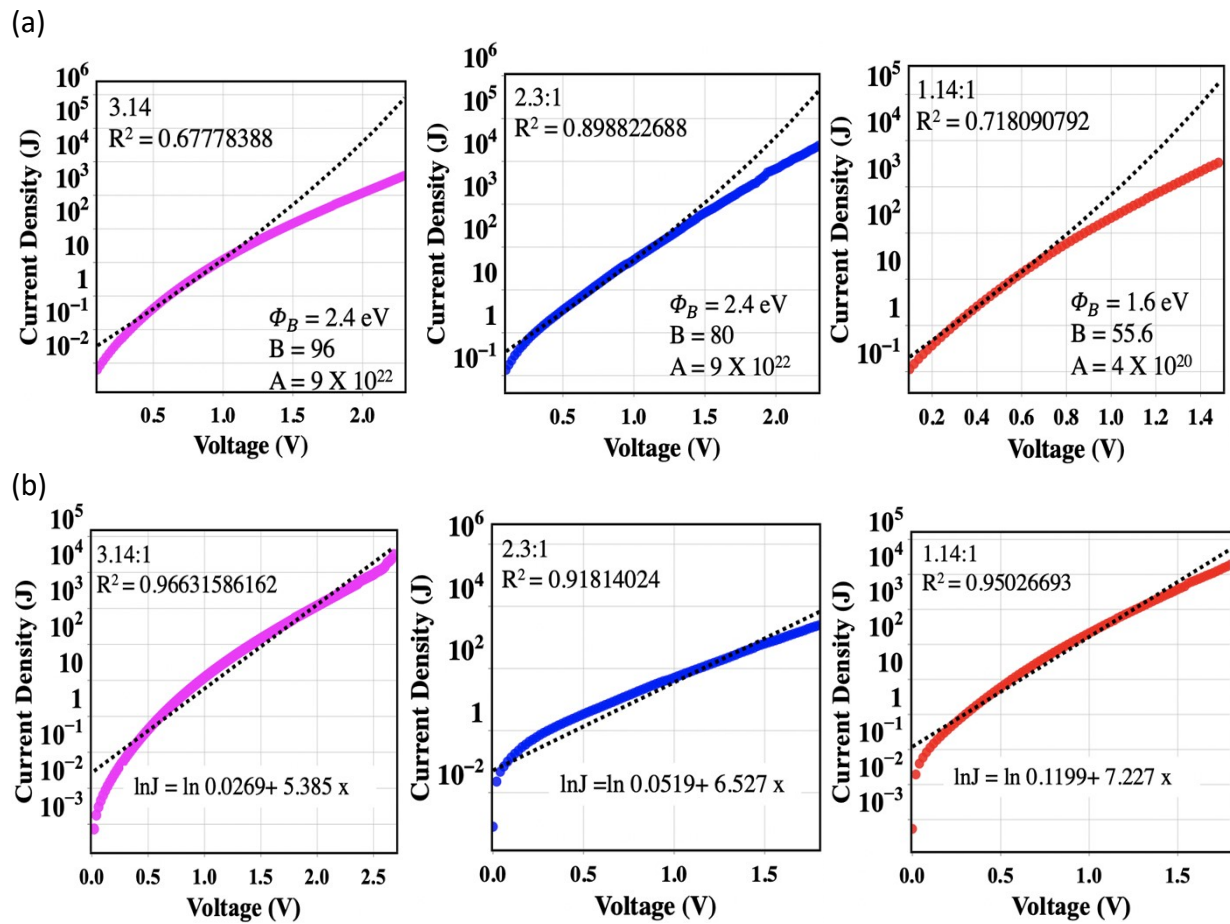
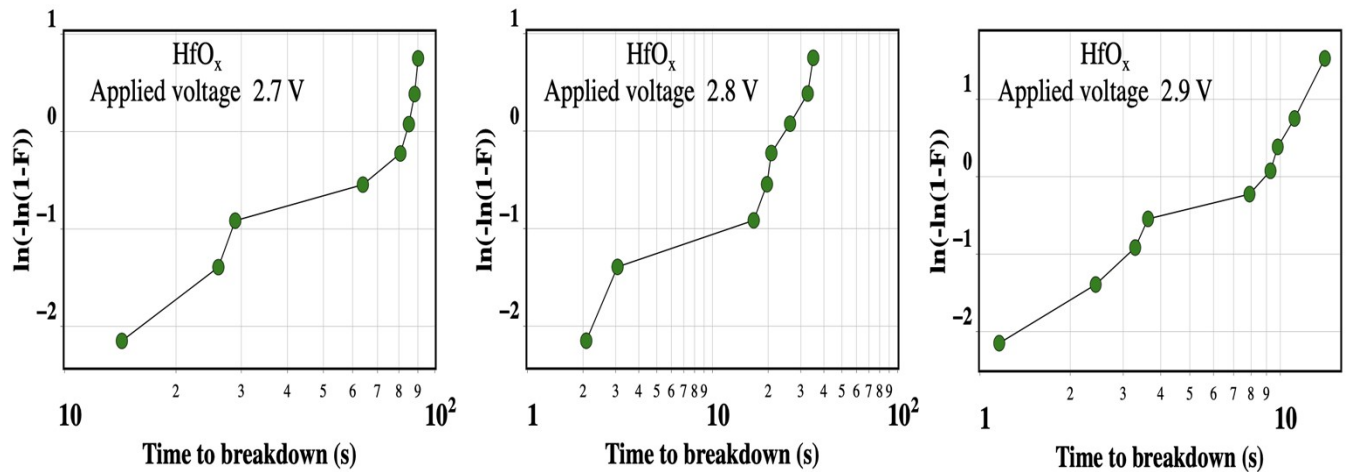


Figure S5: Fitting with the current voltage relationship during forming (a) direct tunneling and (b) trap assisted tunneling model. Samples Hf:Ti = 3.14:1, 2.3:1 and 1.14:1 are representing by magenta, blue and red curves, respectively. Fitting with the both trap-assisted-tunneling and direct tunneling suggest that conduction mechanism is likely trap assisted tunneling.

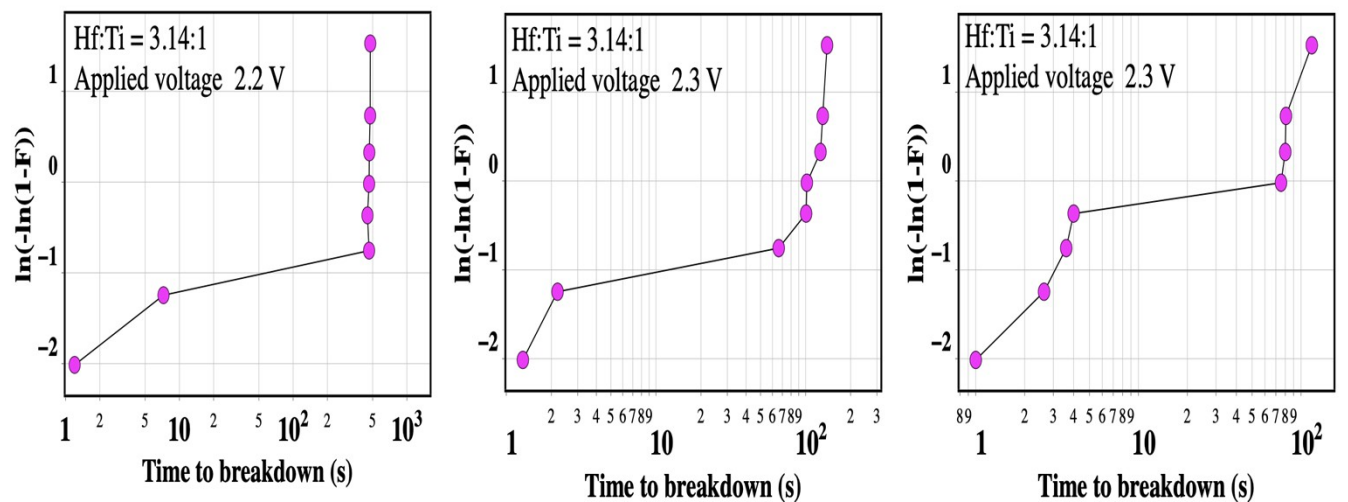
### Weibull statistics of charge-to-breakdown measurement:

in Figure S5 Weibull function distributions are shown for  $\text{HfO}_x$  and  $\text{Hf}_x\text{Ti}_y\text{O}_z$  devices. During breakdown measurement when several identical samples are tested the breakdown voltages distributes over a wide range. For statistical description of such tests Weibull distribution is a widely used.<sup>1</sup> The Weibull function is described through percolation theory which is  $\ln[-\ln(1-F)]$ , where  $F$  is denoted as the cumulative failure rate. Two distinctive slopes will result in the Weibull function as a function of time to breakdown plot. If failure is caused by the extrinsic reasons sample set will show smaller slope in Weibull distribution.<sup>1, 2</sup> On the other hand, regions with higher Weibull distribution slope indicates failure due to intrinsic reason. The time to breakdown at the point where Weibull function value is zero is denoted as modal value.

(a)



(b)



(c)

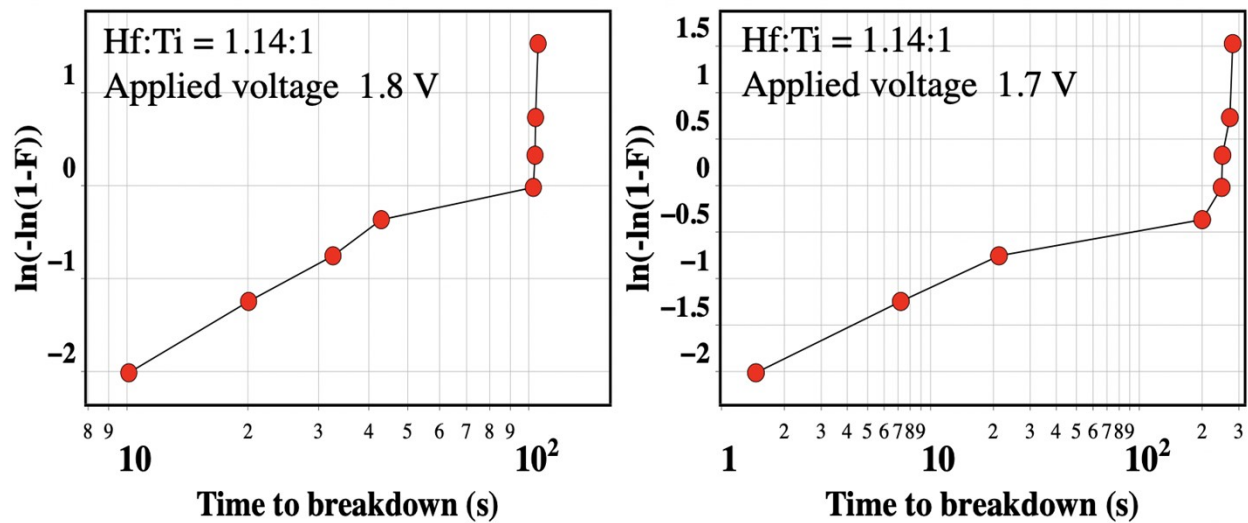
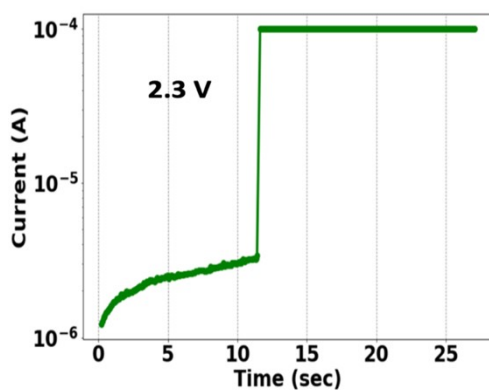


Figure S6: Weibull statistics of the oxides breakdown during forming, (a)  $\text{HfO}_x$ , with modulus values are 83 s, 35 s and 9.2 s for 2.7 V, 2.8 V and 2.9 V respectively. (b)  $\text{Hf:Ti} = 3.14:1$  with modulus values are 513 s, 100 s and 85 s for 2.2 V, 2.3 V and 2.4 V respectively and, (c)  $\text{Hf:Ti} = 1.14:1$  with modal values are 100 s, 212.3 s and 85 s for 1.8 V and 1.7 V respectively.

#### Charge-to-breakdown measurement current time relationship:

Figure S6 shows current and time to dielectric breakdown measurement at two different voltages. Application of a constant voltage leads to breakdown of the dielectric oxide. The charge was calculated from the integration of the current up to the dielectric breakdown which is shown in the main text in Figure 4.

(a)



(b)

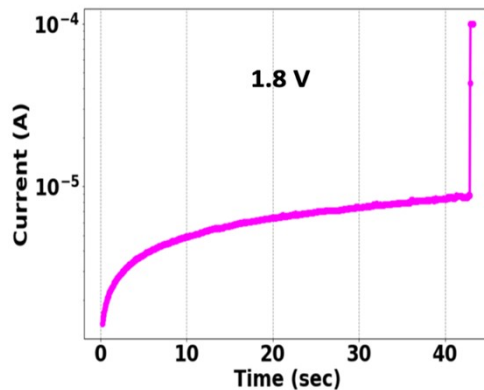
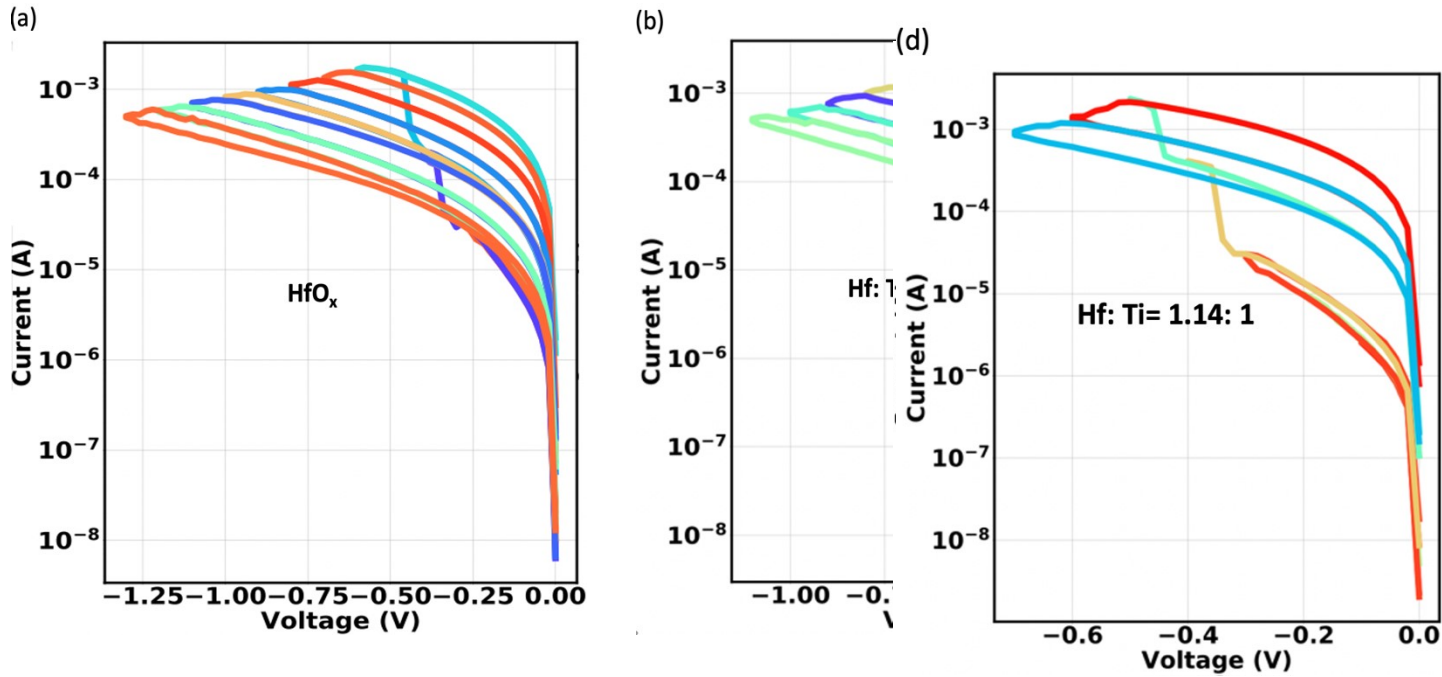
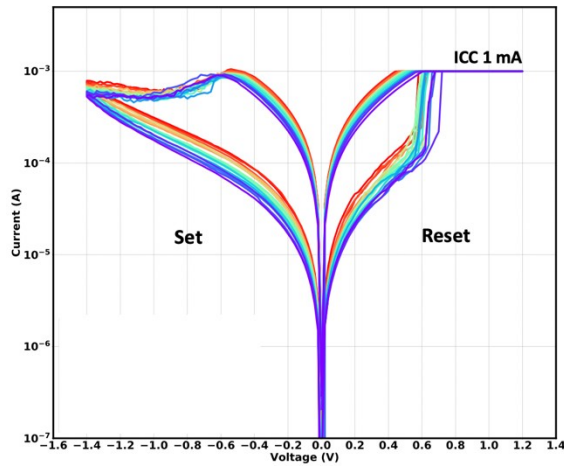


Figure S7: Time-to-dielectric breakdown as a function of current for the devices, (a) gate voltage 2.3 V, and (b) gate voltage 1.8 V. A constant gate voltage was applied at the top electrode. The current and time to breakdown was measured for a given voltage.

**Gradual Reset:** After performing the forming operation, devices were switched to high resistance state (HRS) by applying negative voltages on the top electrode. This operation was performed gradually by applying consecutive reset voltages. For this, reset voltages were applied gradually



(e)



**Figure S8: Current voltage relationship. Gradual reset process for the devices. (a) HfO<sub>x</sub> device, (b) Hf<sub>x</sub>Ti<sub>y</sub>O<sub>z</sub> device with Hf:Ti 3.14:1, (c) Hf<sub>x</sub>Ti<sub>y</sub>O<sub>z</sub> device with Hf:Ti 2.30:1, and (d) Hf<sub>x</sub>Ti<sub>y</sub>O<sub>z</sub> device with Hf:Ti 1.14:1. (e) Typical stabilization set reset loops (~50) for the fabricated devices.**

starting from 0 V to a maximum negative reset stop voltage with an increment of -0.1 V. The maximum reset voltages are dependent on the Titanium content in the oxide. Application of gradual reset voltages ensured controlled motion of oxygen ions across the filament during the reset process. After gradual reset the devices were switched between the LRS and HRS to stabilize the already formed filaments.

**Current-voltage relationship of HfO<sub>x</sub> device with and without the titanium capping layer:**

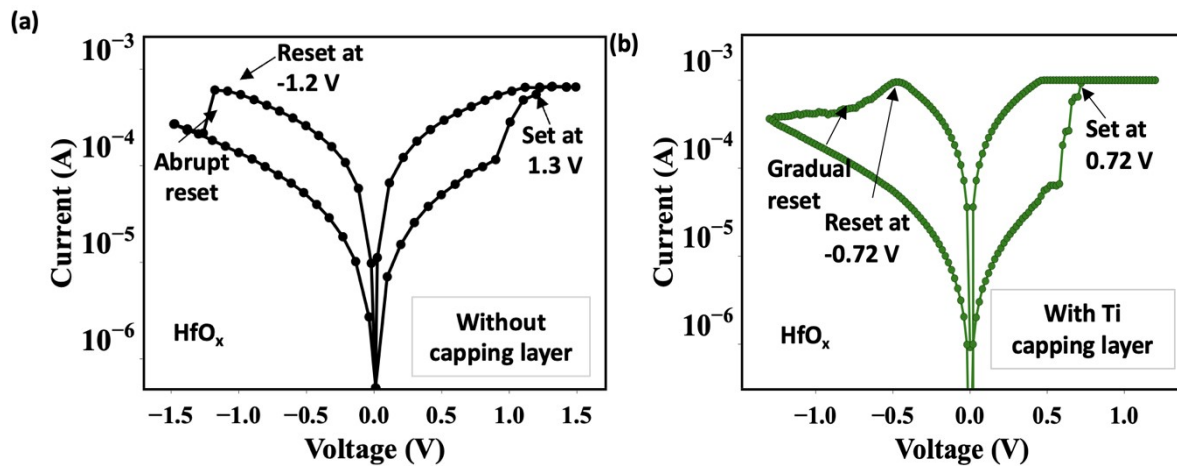


**Figure S9: Current-voltage relationship of HfO<sub>x</sub> device (a) without the Ti capping layer. The set-reset initiation voltages are 1.3 V and -1.2 V, respectively, (b) with the Ti capping layer. The set-reset initiation voltages are 0.72 V and -0.48 V, respectively. The set reset initiation voltages are smaller and the switching window is wider in the device with the Ti capping layer. Moreover, the reset transition is also more gradual in the Ti capping layer device.**

**Table S3:** Suboxide and metallic Ti contents from the XPS Ti 2p spectra deconvolution for Hf:Ti = 3.14:1 and Hf:Ti = 1.14:1 devices

		Hf:Ti = 3.14:1 Device			Hf:Ti = 1.14:1 Device		
		Etch Time: 0 sec					
		B. E. (eV)	Area (%)	Area (%)	B. E. (eV)	Area (%)	Area (%)
Ti(0) or Ti Metal	Ti 2p 3/2	454.0	0.0		453.9	0.0	
	Ti 2p 1/2	460.0	2.9	2.9	460.2	4.2	4.3
Ti(II) or TiO	Ti 2p 3/2	455.9	0.2		456.1	0.2	
	Ti 2p 1/2	461.1	2.4	2.6	460.9	0.5	0.7
Ti(III) or Ti <sub>2</sub> O <sub>3</sub>	Ti 2p 3/2	457.3	3.8		457.3	4.5	
	Ti 2p 1/2	462.3	0.9	4.7	462.4	1.9	6.4
Ti(IV) or TiO <sub>2</sub>	Ti 2p 3/2	458.6	58.2		458.6	58.2	

	Ti 2p 1/2	464.3	31.7	89.8	464.4	30.5	88.7
<b>Total</b>		100.0			100.0		
<b>Etch Time: 5 sec</b>							
		<b>B. E. (eV)</b>	<b>Area (%)</b>	<b>Area (%)</b>	<b>B. E. (eV)</b>	<b>Area (%)</b>	<b>Area (%)</b>
<b>Ti(0) or Ti Metal</b>	Ti 2p 3/2	454.0	0.0		454.0	0.0	
	Ti 2p 1/2	459.9	4.0	4.0	460.2	16.8	16.8
<b>Ti(II) or TiO</b>	Ti 2p 3/2	456.1	3.3		456.1	0.1	
	Ti 2p 1/2	460.9	6.4	9.7	461.2	1.1	1.1
<b>Ti(III) or Ti<sub>2</sub>O<sub>3</sub></b>	Ti 2p 3/2	457.0	9.9		457.3	8.5	
	Ti 2p 1/2	462.4	1.9	11.7	462.3	0.1	8.6
<b>Ti(IV) or TiO<sub>2</sub></b>	Ti 2p 3/2	458.7	48.2		458.6	44.9	
	Ti 2p 1/2	464.5	26.3	74.6	464.5	28.6	73.5
<b>Total</b>		100.0			100.0		
<b>Etch Time: 10 sec</b>							
		<b>B. E. (eV)</b>	<b>Area (%)</b>	<b>Area (%)</b>	<b>B. E. (eV)</b>	<b>Area (%)</b>	<b>Area (%)</b>
<b>Ti(0) or Ti Metal</b>	Ti 2p 3/2	454.0	0.1		454.0	0.1	
	Ti 2p 1/2	459.8	3.4	3.5	460.1	12.2	12.4
<b>Ti(II) or TiO</b>	Ti 2p 3/2	455.6	13.9		456.1	8.8	
	Ti 2p 1/2	461.1	10.8	24.7	461.3	0.9	9.7
<b>Ti(III) or Ti<sub>2</sub>O<sub>3</sub></b>	Ti 2p 3/2	456.9	17.5		457.2	13.3	
	Ti 2p 1/2	462.5	5.4	22.9	462.4	5.5	18.8
<b>Ti(IV) or TiO<sub>2</sub></b>	Ti 2p 3/2	458.7	31.6		458.7	37.1	
	Ti 2p 1/2	464.5	17.2	48.9	464.5	22.0	59.2
<b>Total</b>		100.0			100.0		
<b>Etch Time: 15 sec</b>							
		<b>B. E. (eV)</b>	<b>Area (%)</b>	<b>Area (%)</b>	<b>B. E. (eV)</b>	<b>Area (%)</b>	<b>Area (%)</b>
<b>Ti(0) or Ti Metal</b>	Ti 2p 3/2	454.1	0.1		454.0	0.5	
	Ti 2p 1/2	459.8	5.8	5.9	460.0	11.9	12.4
<b>Ti(II) or TiO</b>	Ti 2p 3/2	455.5	22.6		455.7	14.3	
	Ti 2p 1/2	461.2	11.5	34.1	461.3	2.5	16.8
<b>Ti(III) or Ti<sub>2</sub>O<sub>3</sub></b>	Ti 2p 3/2	457.1	17.1		457.1	14.3	
	Ti 2p 1/2	462.4	6.1	23.1	462.4	7.4	21.7
<b>Ti(IV) or TiO<sub>2</sub></b>	Ti 2p 3/2	458.7	22.6		458.7	31.9	
	Ti 2p 1/2	464.4	14.3	36.9	464.5	17.3	49.2
<b>Total</b>		100.0			100.0		

Reference:

1. Wu, E.; Nowak, E.; Vayshenker, A.; McKenna, J.; Harmon, D.; Vollertsen, R.-P., New global insight in ultrathin oxide reliability using accurate experimental methodology and comprehensive database. *IEEE transactions on device and materials reliability* **2001**, 1 (1), 69-80.

2. Degraeve, R.; Ogier, J.-L.; Bellens, R.; Roussel, P.; Groeseneken, G.; Maes, H., A new model for the field dependence of intrinsic and extrinsic time-dependent dielectric breakdown. *IEEE Transactions on Electron Devices* **1998**, *45* (2), 472-481.